MATHEMATICAL MODELING AND COMPUTING, Vol. 11, No. 4, pp. 1118–1127 (2024)

Effect of nanoparticle shape on natural convection in hybrid nanofluid inside square cavity

Mohd Ali Hanafiah M. A.[1], Ab Ghani A.[1*], Hafidzuddin M. E. H.[1,2], Md Arifin N.[1*], Mohamad Som M. N.[1,2]

[1] *Department of Mathematics and Statistics, Universiti Putra Malaysia, 43400 Serdang, Selangor, Malaysia*

[2] *Centre for Foundation Studies in Science of Universiti Putra Malaysia, 43400 Serdang, Selangor, Malaysia*

[*] *Corresponding authors: norihana@upm.edu.my, aniza@upm.edu.my*

(Received 16 July 2024; Revised 25 November 2024; Accepted 26 November 2024)

A numerical study of natural convection in a square cavity with Al_2O_3-Cu/water hybrid nanofluid, focusing on the effects of nanoparticle shape, is conducted. The governing partial differential equations and corresponding boundary conditions are transformed into nondimensional forms and solved using the finite element method. The flow and heat transfer characteristics are graphically illustrated and explained for different nanoparticle volume fractions and shapes, with corresponding average Nusselt numbers. It has been observed that a variety of nanoparticle shapes effect, as the empirical nanoparticle shape factor m increases, the total surface area of the nanoparticle increases. This causes more heat can be dissipated and in turn, produces a higher heat transfer rate.

Keywords: *natural convection flow; Al_2O_3-Cu/water hybrid nanofluid; square cavity; finite element method; nanoparticle shape.*

2010 MSC: 35Q35, 80A20, 65L10, 34K10 **DOI:** 10.23939/mmc2024.04.1118

1. Introduction

Natural convection in closed cavities is one of the most important subjects of fluid flow and heat transfer. This subject has received much attention due to many energy-related applications, such as heat transfer in buildings, nanofluid heat transfer enhancement and control, solar energy collectors, semiconductor manufacturing, and nuclear energy management. The motion of the fluid in natural convection occurs due to the buoyancy forces imposed on the fluid when its density of the heat transfer surface is described as a result of thermal expansion of the fluid in a non-uniform temperature distribution. Most authors considered the flow and heat transfer inside a square or rectangular cavity because the numerical solution is not complicated, and the geometry is very simple to simulate.

Nanofluids are used in various heat transfer applications. Different nano sized particles such as Al_2O_3, Cu, CuO, SO_2, TiO_2 are added in the base fluid to enhance the thermal characteristics of the base flow. Many studies have modeled and simulated the natural convection of a suspension of nanoparticles in a base fluid in cavity. Hashim et al. [1] and Alsabery et al. [2] investigated the flow and heat transfer of nanofluids in a wavy wall cavity. Tahmasebi et al. [3] and Ghalambaz et al. [4] and studied the effect of the presence of a layer of porous media and a layer of a solid wall on the flow and natural convection heat transfer of nanofluids. The influence of thermal radiation on entropy generation within a closed cavity filled with Al_2O_3-water was investigated in the numerical study of Zhang et al. [5]. Sedeghi et al. [6] reviewed and summarized the findings of the published literature on enhancement of natural convection in various enclosures filled using nanofluid. Nazir et al. [7] studied the effect of radiation and heat generation on natural convection flow of nanofluid inside the triangular cavity.

Hybrid nanofluids have been the subject of many scientific works in past decades. The hybrid nanofluids is a mixture of two kinds of solid nanoparticles in a base fluid to improve the thermophysical properties of single type of solid nanoparticle. The Al_2O_3-Cu/water hybrid nanofluid also has a higher heat transfer rate than the Al_2O_3/water nanofluid, as reported by Olatundun and Makinde [8]. Revnic et al. [9] investigated the MHD natural convection effects inside the discrete heating wavy cavity filled with hybrid-nanofluid with particles. Recently, several articles have reported the enhancement of energy transport processes through hybrid nanofluids [10–15]. It was found that the heat transfer rate of the hybrid nanofluid is superior to the Cu/water nanofluid. Besides that, it was observed that the highest increment of Nusselt number was achieved in the use of blade-shaped nanoparticles, compared to the platelet, cylindrical, brick, and spherical shapes.

Based on the previous works, the present study the effects of nanoparticles shape on natural convection in a square cavity with Al_2O_3-Cu/water hybrid nanofluid. To our best knowledge this problem has not been analyzed yet. The proposed problem aims to provide beneficial information on the efficiency of hybrid nanofluid and shapes of nanoparticles in the flow containing the assumed conditions, which may present in the manufacturing or engineering processes.

2. Problem formulation

In this study, a square cavity was used to assess how its thermal system performs, its reactivity to heat transfer, and its thermal conductivity on natural convection. The Rayleigh number had a substantial influence on the flow profile and heat transmission within the cavity, as well as the thickness of the thermal barrier layer, in a square form. The enclosure is a square with the hot wall $EFGJ$, the top wall BC is cooled with a constant temperature T_c and the hot wall $EFGJ$ is heated with a constant temperature T_h, where $T_h > T_c$ as shown in Figure 1. The walls AB, CD, DE, and JA are thermally insulated. The enclosure is filled with Cu-Al_2O_3-H_2O hybrid nanofluid.

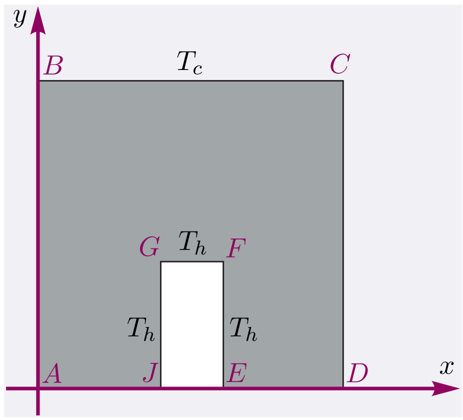

Fig. 1. Physical model.

The governing equations of Navier–Stokes and energy examine steady, two-dimensional viscous incompressible flow are written. The following dimensional system of equations for hybrid nanofluid:

$$\frac{\partial u}{\partial x} + \frac{\partial v}{\partial y} = 0, \tag{1}$$

$$u\frac{\partial u}{\partial x} + v\frac{\partial u}{\partial y} = \frac{1}{\rho_{hnf}}\frac{\partial p}{\partial x} + \frac{\mu_{hnf}}{\rho_{hnf}}\left(\frac{\partial^2 u}{\partial x^2} + \frac{\partial^2 u}{\partial y^2}\right), \tag{2}$$

$$u\frac{\partial v}{\partial x} + v\frac{\partial v}{\partial y} = \frac{1}{\rho_{hnf}}\frac{\partial p}{\partial x} + \frac{\mu_{hnf}}{\rho_{hnf}}\left(\frac{\partial^2 v}{\partial x^2} + \frac{\partial^2 v}{\partial y^2}\right) + \frac{(\rho\beta)_{hnf}}{\rho_{hnf}} g\left(T - T_c\right), \tag{3}$$

$$u\frac{\partial T}{\partial x} + v\frac{\partial T}{\partial y} = \alpha\left(\frac{\partial^2 T}{\partial x^2} + \frac{\partial^2 T}{\partial y^2}\right). \tag{4}$$

The boundary conditions:
at all surfaces:

$$U = V = 0, \tag{5}$$

at AB, CD, EF and GJ:

$$\frac{\partial U}{\partial Y} = 0, \tag{6}$$

at BC, DE, FG, and JA:

$$\frac{\partial V}{\partial X} = 0. \tag{7}$$

The thermal properties of base fluid and empirical correlation for hybrid nanofluid is given in Table 1 [4]. The thermophysical properties of water and solid hybrid nanoparticles Alumina (Al_2O_3)

and Copper (Cu) are stated in Table 2 and the nanoparticle empirical shape factor is mentioned in Table 3 where m is the shape factor.

Table 1. Thermophysical properties correlations.

Properties	**Hybrid Nanofluid Correlations**
Density	$\rho_{hnf} = \varphi_{\mathrm{Al_2O_3}}\rho_{Al_2O_3} + \varphi_{Cu}\rho_{Cu} + (1-\varphi)\,\rho_f$, where $\varphi_{hnf} = \varphi_{\mathrm{Al_2O_3}} + \varphi_{\mathrm{Cu}}$
Heat capacity	$(\rho C_p)_{hnf} = \varphi_{\mathrm{Al_2O_3}}\,(\rho C_p)_{\mathrm{Al_2O_3}} + \varphi_{\mathrm{Cu}}\,(\rho C_p)_{Cu} + (1-\varphi)\,(\rho C_p)_f$
Dynamic Viscocity	$\mu_{hnf} = \mu_f\,(1-\varphi_{\mathrm{Al_2O_3}} - \varphi_{\mathrm{Cu}})^{-2.5}$
Thermal Diffusivity	$\alpha_{hnf} = \frac{k_{hnf}}{(\rho C_p)_{hnf}}$
Thermal Conductivity	$\frac{k_{hnf}}{k_f} = \frac{\left[\left(\frac{\varphi_{\mathrm{Al_2O_3}}k_{\mathrm{Al_2O_3}}+\varphi_{\mathrm{Cu}}k_{\mathrm{Cu}}}{\varphi}\right)+(m-1)k_f-(m-1)\ \varphi\left(k_f-\left(\frac{\varphi_{\mathrm{Al_2O_3}}k_{\mathrm{Al_2O_3}}+\varphi_{\mathrm{Cu}}k_{\mathrm{Cu}}}{\varphi}\right)\right)\right]}{\left[\left(\frac{\varphi_{\mathrm{Al_2O_3}}k_{\mathrm{Al_2O_3}}+\varphi_{\mathrm{Cu}}k_{\mathrm{Cu}}}{\varphi}\right)+(m-1)k_f-\ \varphi\left(k_f-\left(\frac{\varphi_{\mathrm{Al_2O_3}}k_{\mathrm{Al_2O_3}}+\varphi_{\mathrm{Cu}}k_{\mathrm{Cu}}}{\varphi}\right)\right)\right]}$
Electrical Conductivity	$\frac{\sigma_{hnf}}{\sigma_f} = \frac{\left[\left(\frac{\varphi_{\mathrm{Al_2O_3}}\sigma_{\mathrm{Al_2O_3}}+\varphi_{\mathrm{Cu}}\sigma_{\mathrm{Cu}}}{\varphi}\right)+2\sigma_f+2\left(\varphi_{\mathrm{Al_2O_3}}\sigma_{\mathrm{Al_2O_3}}+\varphi_{\mathrm{Cu}}\sigma_{\mathrm{Cu}}\right)-2\varphi\sigma_f\right]}{\left[\left(\frac{\varphi_{Al_2O_3}\sigma_{Al_2O_3}+\varphi_{Cu}\sigma_{Cu}}{\varphi}\right)+2\sigma_f-\left(\varphi_{Al_2O_3}\sigma_{Al_2O_3}+\varphi_{Cu}\sigma_{Cu}\right)+\varphi\sigma_f\right]}$
Thermal Expansion	$(\rho\beta)_{hnf} = \varphi_{\mathrm{Al_2O_3}}\,(\rho\beta)_{\mathrm{Al_2O_3}} + \varphi_{\mathrm{Cu}}\,(\rho\beta)_{\mathrm{Cu}} + (1-\varphi)\,(\rho\beta)_f$

Table 2. Thermophysical properties.

Properties	**Water (H_2O)**	**Alumina (Al_2O_3)**	**Copper (Cu)**
ρ (kg/m^3)	997.1	3970	8933
C_p (J/kg K)	4179	765	385
k (W/mK)	0.613	40	400
ρ (S/m)	5.5×10^{-6}	35×10^{6}	59.6×10^{6}
β (1/K)	21×10^{-5}	0.85×10^{-5}	1.67×10^{-5}
Pr	6.2		
α	1.47×10^{-7}		

Table 3. Nanoparticle empirical shape.

Shape	**Shape Factor**
Sphere	3
Cube/brick	3.7
Cylindrical	4.9

Here, μ_{hnf}, ρ_{nhf}, k_{hnf}, and $(\rho\ C_p)_{hnf}$ are the dynamic viscosity, density, thermal conductivity, and heat capacity of the hybrid nanofluid, respectively, φ_{hnf} is the nanoparticle volume fraction ($\varphi = 0$ corresponds to a regular heat transfer fluid, $\varphi_{\mathrm{Al_2O_3}}$ for Al_2O_3 nanoparticle and φ_{Cu} for Cu nanoparticle), the suffix f is for water, and C_p is the heat capacity at constant pressure.

Considering the following parameters;

$$(X,Y) = \frac{(x,y)}{L}, \quad (U,V) = \frac{(uL,vL)}{\alpha_{hnf}}, \quad P = \frac{pL^2}{\rho_j\alpha_{hnf}^2}, \quad \theta = \frac{(T-T_c)}{(T_h-T_c)}. \tag{8}$$

The governing equations (1)–(4) are reduced to the following set of dimensionless equation:

$$U\frac{\partial U}{\partial X} + V\frac{\partial U}{\partial Y} = -\frac{\partial P}{\partial X} + \mathrm{Pr}\frac{\nu_{hnf}}{\nu_f}\left(\frac{\partial^2 U}{\partial X^2} + \frac{\partial^2 U}{\partial Y^2}\right), \tag{9}$$

$$U\frac{\partial V}{\partial X} + V\frac{\partial V}{\partial Y} = -\frac{\partial P}{\partial X} + \mathrm{Pr}\frac{\nu_{hnf}}{\nu_f}\left(\frac{\partial^2 V}{\partial X^2} + \frac{\partial^2 V}{\partial Y^2}\right) + \frac{(\rho\beta)_{hnf}}{\rho_{hnf}\beta_f}\,\mathrm{Pr}\,\mathrm{Ra}\,\theta, \tag{10}$$

$$U\frac{\partial \theta}{\partial X} + V\frac{\partial \theta}{\partial Y} = \frac{\alpha_{hnf}}{\alpha_f}\left(\frac{\partial^2 \theta}{\partial X^2} + \frac{\partial^2 \theta}{\partial Y^2}\right), \tag{11}$$

where $\mathrm{Pr} = \frac{\mu_f(\rho C_p)_f}{\rho_f k_f}$ is the Prandtl number and $\mathrm{Ra} = \frac{g(\rho\beta)_f(T_h-T_c)(\rho C_p)_f L^3}{\mu_f k_f}$ is the Rayleigh number.

The corresponding non-dimensional boundary conditions are:
at BC:

$$\theta = 0, \tag{12}$$

at EF, FG and GJ:

$$\theta = 1, \tag{13}$$

at AB and CD:

$$\frac{\partial \theta}{\partial X} = 0, \tag{14}$$

at DE and JA:

$$\frac{\partial \theta}{\partial Y} = 0. \tag{15}$$

3. Computational procedure

The Galerkin weighted residual technique accompanying with the finite element method do apply to investigate the control equations of Eqs. (9)–(11). The governing Eqs. (9)–(11) along with the associated boundary condition (13)–(15) is solved using the Galerkin weighted residual along with finite element method. Alsabery et al. [16] has been thoroughly examined and approved this method. Figure 2 displays the problem's finite element mesh. Five different finite element meshes have been considered and the value of Nu_{avg} are carried out and presented in Table 4. Therefore, all the simulations have been carried out at mesh size extra fine with 22428 elements grid system. The iteration is reported until the normalized residual of the governing equations less than 10^{-6}.

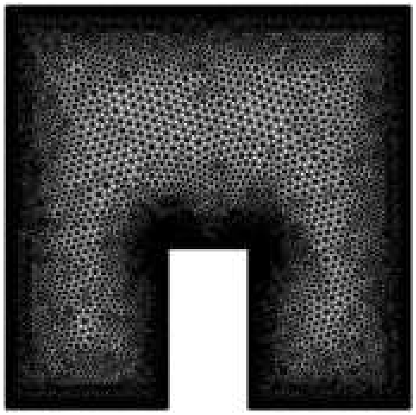

Fig. 2. Example of mesh generation.

Table 4. Comparison for different type of mesh size.

Predefined mesh size	**Domain elements**	**Boundary elements**	Nu_{avg}	**CPU time (s)**
Normal	2163	159	15.445	14
Fine	3466	198	15.607	14
Finer	8680	402	15.935	20
Extra fine	22428	772	16.109	49
Extremely fine	30254	772	16.106	81

4. Results and discussion

The steady-state results presented in this work are generated for different pertinent dimensionless groups: Rayleigh number ($10^3 \leqslant \mathrm{Ra} \leqslant 10^5$), $W = 0.2$, $H = 0.4$. The default parameters are assigned values unless otherwise stated. Figures 3 to 5 show contours of stream function (streamlines) and temperature (isotherms) with $\mathrm{Pr} = 6.2$, $\varphi_{hnf} = 0.02$, $W = 0.2$, $D = 0.4$ and $H = 0.4$ for different values of the Rayleigh number and nanoparticle shape. For low Ra value, the streamlines are characterized by two symmetrical counter-rotating vortexes occupying the entire cavity body. The corresponding isotherms are mostly parallel to the vertical walls except along the top surface of the heater. The contribution of convection is noticeable at high Ra as evident by the departure of the isotherms from the vertical pattern. As Ra increases to $\mathrm{Ra} = 10^5$, convection mechanism becomes more pronounced and consequently the central vortex moves upward (Figure 5a). Figures 3b to 5b shows that the isotherms are horizontal inside the very thin boundary layers. This can be attributed to high convection current within the cavity which also causes a reduction in the temperature gradients in the centre of the cavity. Figure 6 presents the variations of Nu_{avg} for different Rayleigh Numbers with different nanoparticle shapes at $H = 0.4$ and $\varphi_{hnf} = 0.02$. From Figure 6, the value of Nu_{avg} increases as Ra increases with sphere ($m = 3$) being the lowest and cylindrical ($m = 4.9$) being the highest. As the empirical nanoparticle shape factor increase, the total surface area of the nanoparticle increases. This cause more heat can be dissipated and in turns, produces a higher heat transfer rate.

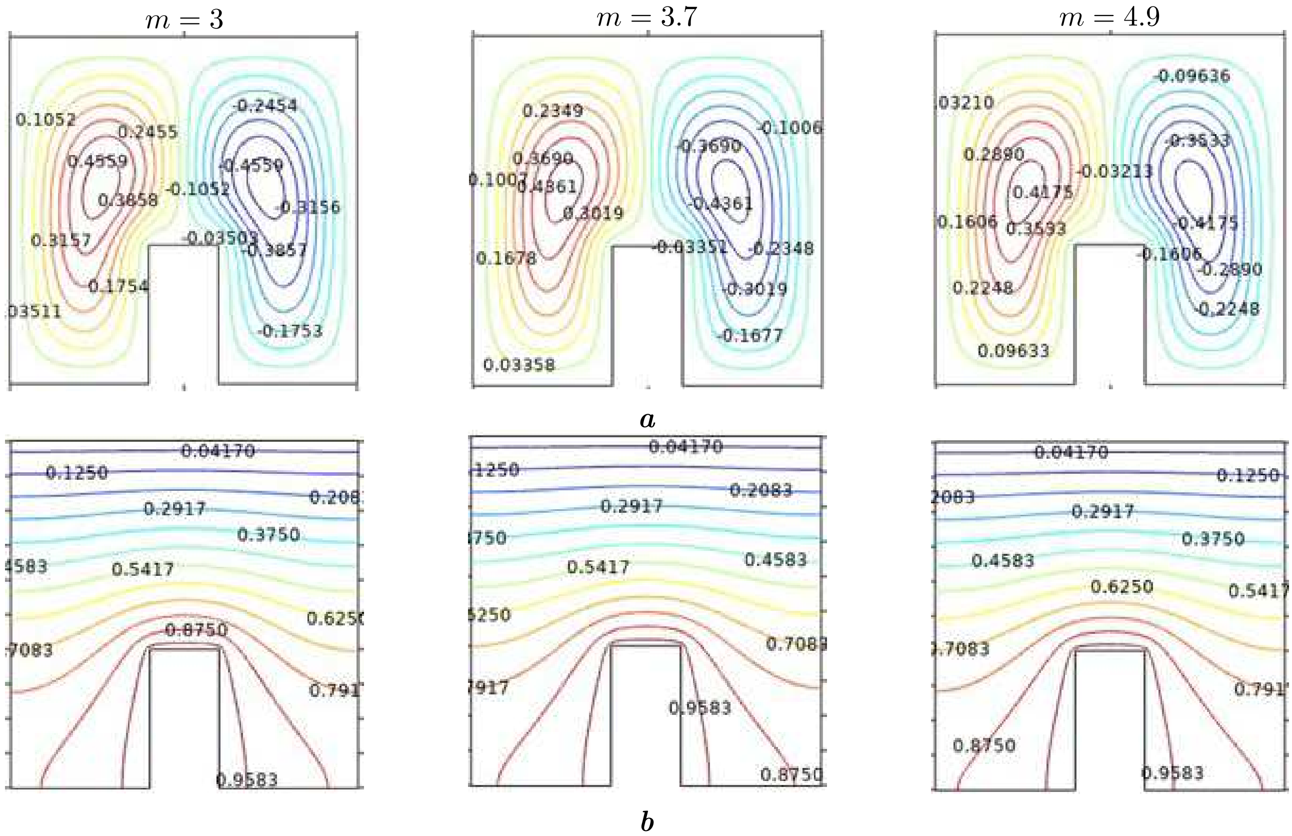

Fig. 3. (*a*) Streamlines and (*b*) isotherms for Ra = 10 000.

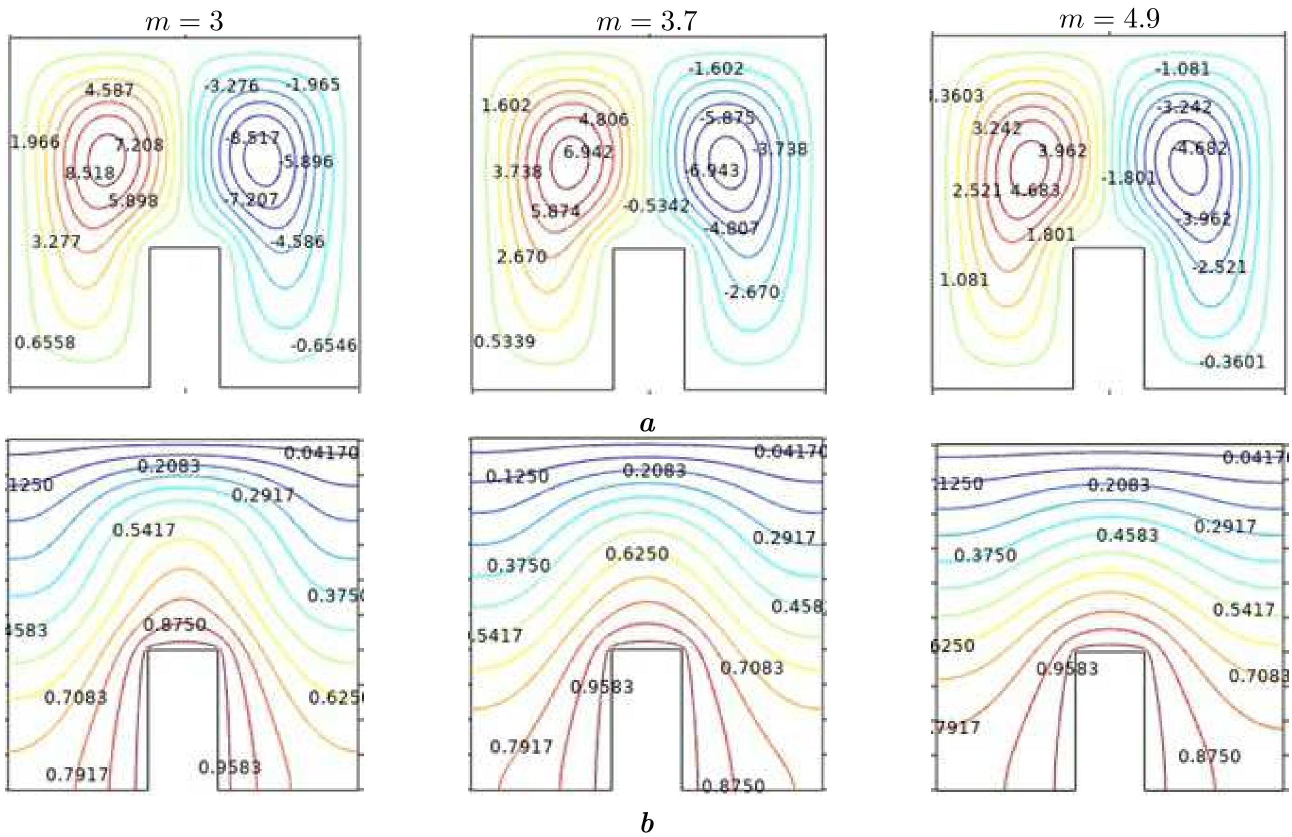

Fig. 4. (*a*) Streamlines and (*b*) isotherms for Ra = 50 000.

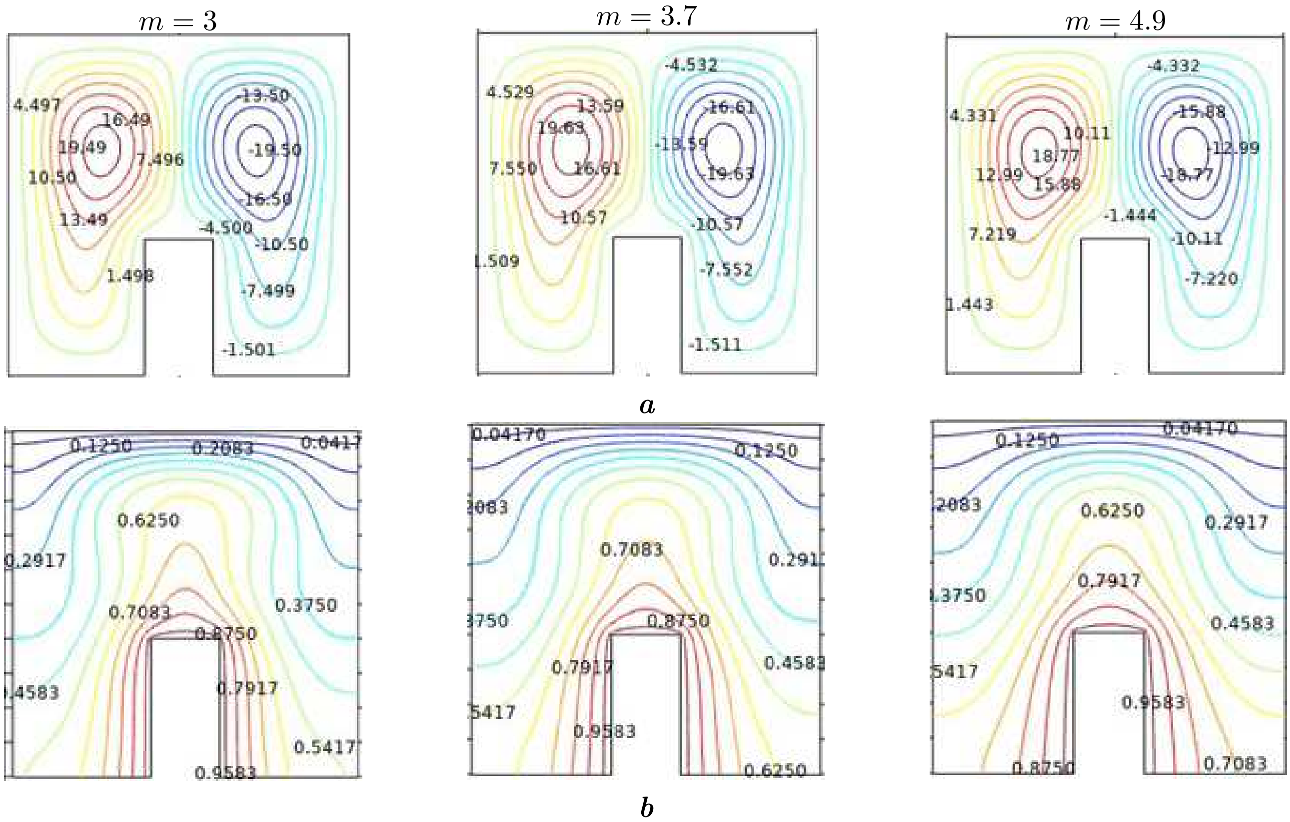

Fig. 5. (*a*) Streamlines and (*b*) isotherms for Ra $= 100\,000$.

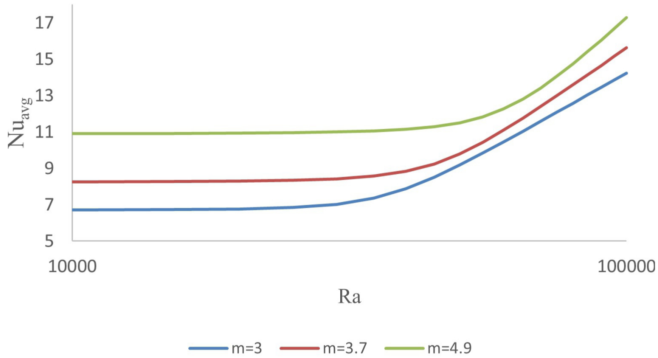

Fig. 6. Variations of the average Nusselt number with Rayleigh number and nanoparticle shape.

Figures 7–9 show the streamlines and isotherms at $\mathrm{Ra} = 10^4$ for the Cu-Al_2O_3 hybrid nanofluid with $\varphi_{hnf} = 0.02$, $\varphi_{hnf} = 0.035$ and $\varphi_{hnf} = 0.05$, respectively. We found that symmetrical behaviour in both the streamlines and the contour maps of the isotherms due to the temperature distribution imposed at the bottom wall and the boundary conditions on vertical walls. The flow is mostly formed of two counter-rotating circulation cells, as shown by the Ra and the value of the solid volume fraction. When the solid volume fraction of nanoparticles increases, the fluid travels slower in the container. The presence of nanoparticles has a significant impact on the heat transfer rate through the enclosure. The heat transmission in this scenario is greatest at $\varphi_{hnf} = 0.05$ and is increased by the presence of nanoparticles, which have a substantially higher thermal conductivity than water. Figure 10 presents the variations of Nu_{avg} for different solid volume fraction and nanoparticle shapes at $H = 0.4$ and $\mathrm{Ra} = 10^4$. It is found that cylindrical ($m = 4.9$) nanoparticle shape produces the highest heat transfer rate while sphere ($m = 3$) is the lowest. The unusual behavior of Nu_{avg} for lower φ_{hnf} is suspected due to the shape of enclosure, the heating and cooling position and the aspect ratio of the cold wall or hot wall.

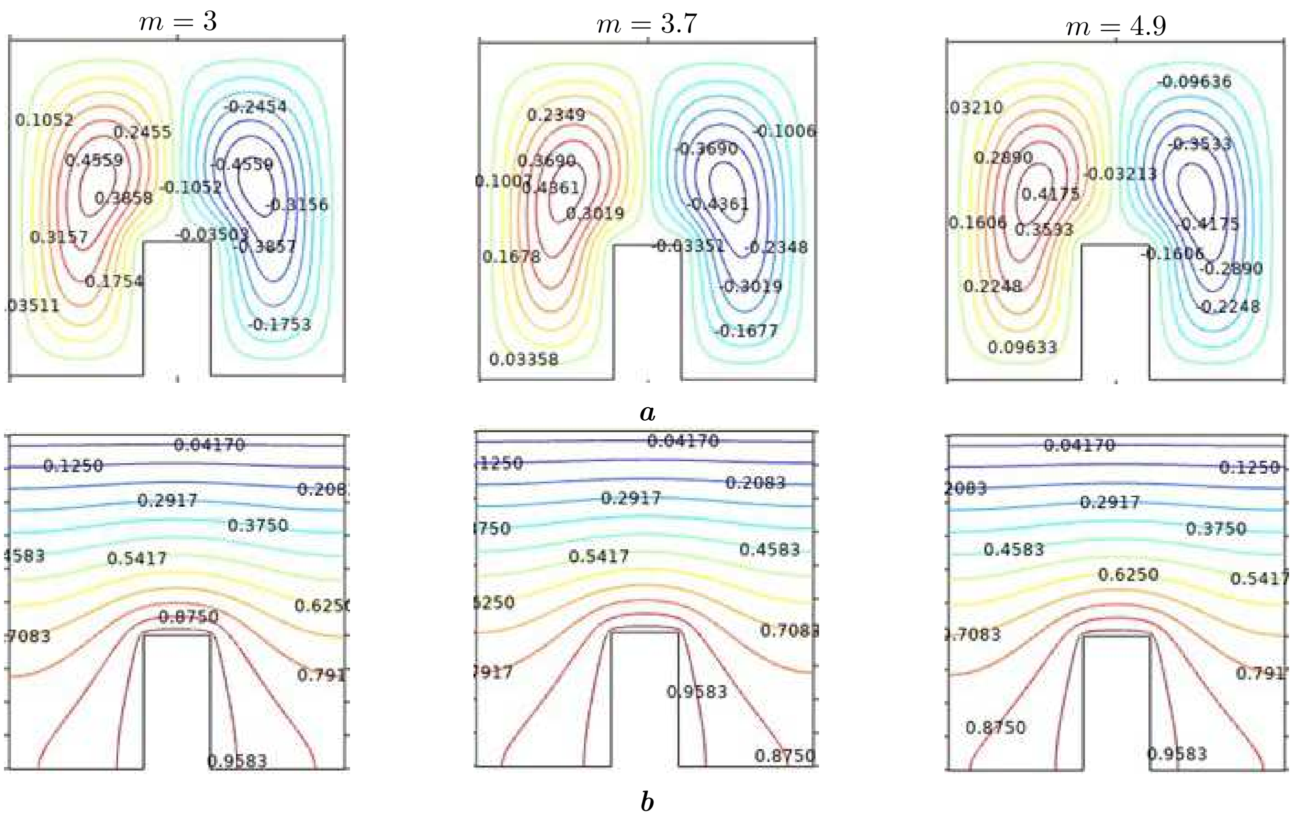

Fig. 7. (***a***) Streamlines and (***b***) isotherms for $\varphi_{hnf} = 0.02$.

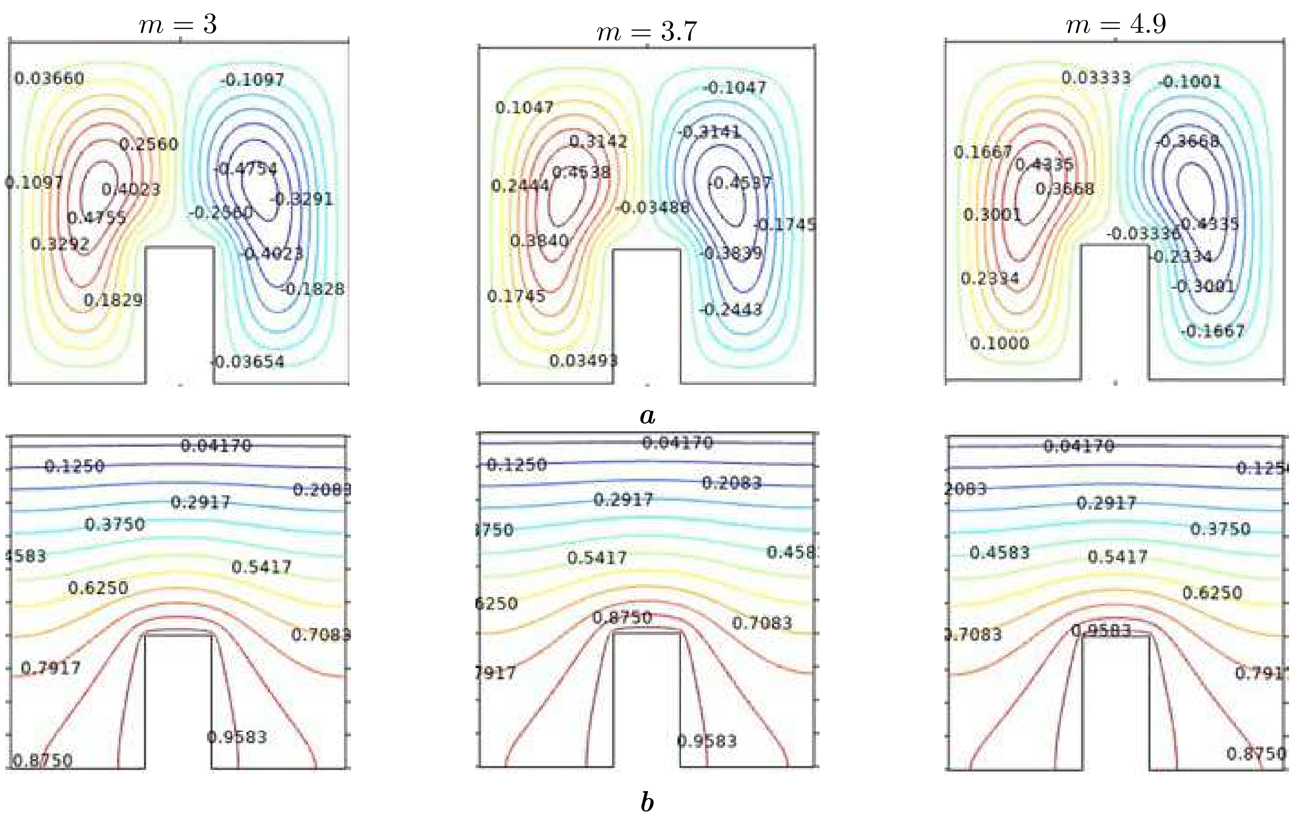

Fig. 8. (***a***) Streamlines and (***b***) isotherms for $\varphi_{hnf} = 0.035$.

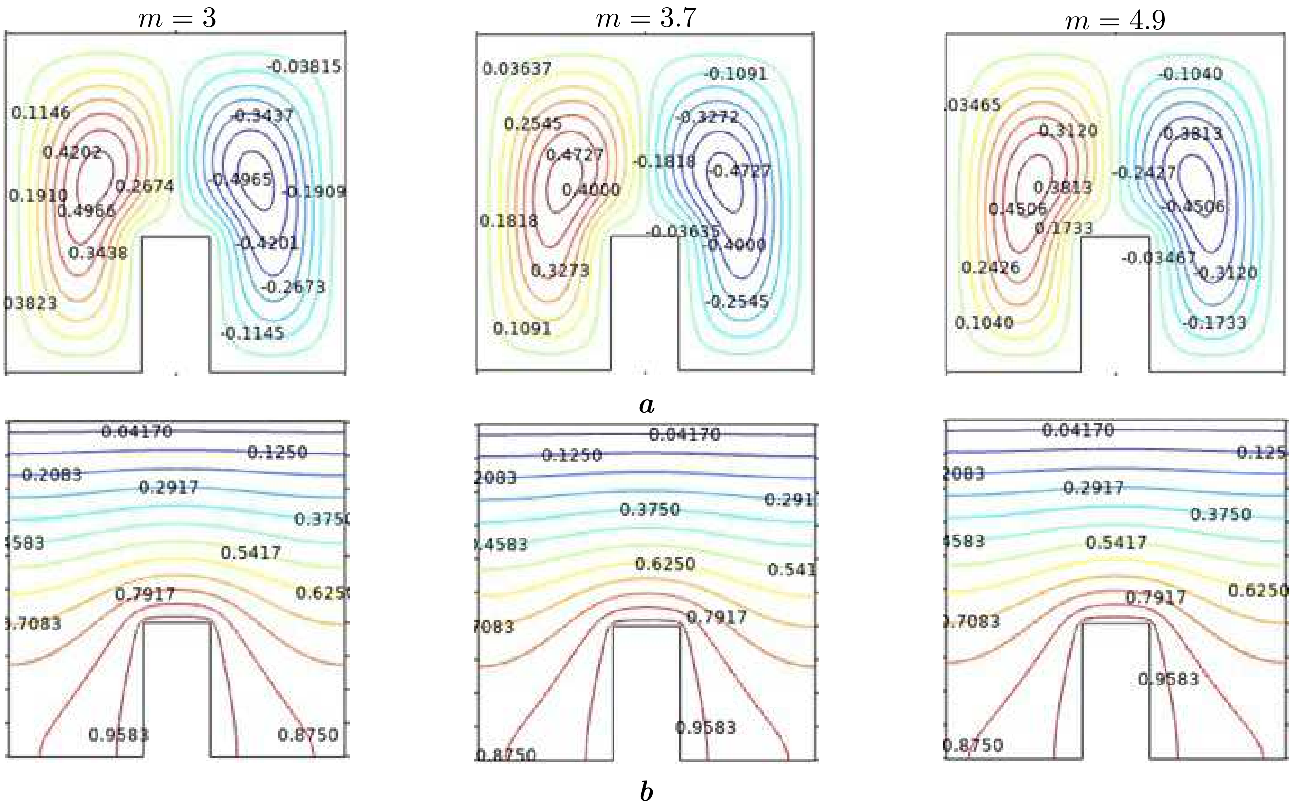

Fig. 9. (***a***) Streamlines and (***b***) isotherms for $\varphi_{hnf} = 0.05$.

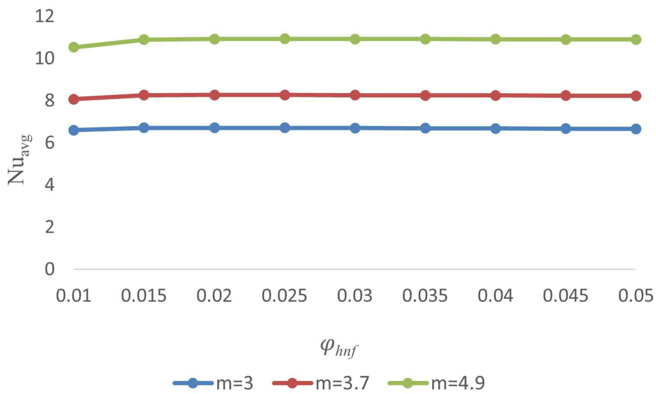

Fig. 10. Variations of the average Nusselt number with nanoparticle volume fraction and nanoparticle shape.

5. Conclusions

In this paper, the effect of nanoparticle shape on natural convection using hybrid nanofluid inside a square cavity was investigated. The average Nusselt number was calculated by deriving numerical solutions for various factors from associated formulation research. The numerical results are presented both graphically and in tabular form for specific parameter values. Hence, the findings of this study can be summarized as follows:

— With the increase in Ra, both Nu_{avg} and heat transfer increase.
— As the nanoparticle shape factor increases, the overall surface area grows, allowing for greater heat dispersion.
— As the solid volume fraction increases, the values of Nu_{avg} increase significantly.
— As a result, the cylindrical nanoparticle shape enhances heat transfer the most, compared to cube and spherical shapes.

[1] Hashim I., Alsabery A., Sheremet M., Chamkha A. Numerical investigation of natural convection of Al_2O_3-water nanofluid in a wavy cavity with conductive inner block using Buongiornos two-phase model. Advanced Powder Technology. **30** (2), 399–414 (2019).

[2] Alsabery A., Sheremet M., Chamkha A., Hashim I. Impact of nonhomogeneous nanofluid model on transient mixed convection in a double lid-driven wavy cavity involving solid circular cylinder. International Journal of Mechanical Sciences. **150**, 637–655 (2019).

[3] Ali Tahmasebi M. M., Ghalambaz M. Local thermal nonequilibrium conjugate natural convection heat transfer of nanofluids in a cavity partially filled with porous media using Buongiorno's model. Numerical Heat Transfer, Part A: Applications. **73** (4), 254–276 (2018).

[4] Ghalambaz M., Sheremet M. A., Mehryan S. A. M., Kashkooli F. M., Pop I. Local thermal non-equilibrium analysis of conjugate free convection within a porous enclosure occupied with Ag-MgO hybrid nanofluid. Journal of Thermal Analysis and Calorimetry. **135** (2), 1381–1398 (2019).

[5] Zhang R., Ghasemi A., Barzinjy A. A., Zareei M., Hamad S. M., Afrand M. Simulating natural convection and entropy generation of a nanofluid in an inclined enclosure under an angled magnetic field with a circular fin and radiation effect. Journal of Thermal Analysis and Calorimetry. **139** (6), 3803–3816 (2020).

[6] Sadeghi M. S., Anadalibkhah N., Ghasemiasl R., Armaghani T., Dogonchi A. S., Chamkha A. J., Ali H., Asadi A. On the natural convection of nanofluids in diverse shapes of enclosures: an exhaustive review. Journal of Thermal Analysis and Calorimetry. **147** (1), 1–22 (2022).

[7] Nazir M. W., Javed T., Ali N., Nazeer M. Effects of radiative heat flux and heat generation on magnetohydodynamics natural convection flow of nanofluid inside a porous triangular cavity with thermal boundary conditions. Numerical Methods for Partial Differential Equations. **40** (2), e22768 (2024).

[8] Olatundun A. T., Makinde O. D. Analysis of Blasius Flow of Hybrid Nanofluids over a Convectively Heated Surface. Defect and Diffusion Forum. **377**, 29–41 (2017).

[9] Revnic C., Groşan T., Sheremet M., Pop I. Numerical simulation of MHD natural convection flow in a wavy cavity filled by a hybrid Cu-Al_2O_3-water nanofluid with discrete heating. Applied Mathematics and Mechanics. **41** (9), 1345–1358 (2020).

[10] Hayat T., Nadeem S. Heat transfer enhancement with Ag-CuO/water hybrid nanofluid. Results in Physics. **7**, 2317–2324 (2017).

[11] Tayebi T., Chamkha A. J. Magnetohydrodynamic Natural Convection Heat Transfer of Hybrid Nanofluid in a Square Enclosure in the Presence of a Wavy Circular Conductive Cylinder. Journal of Thermal Science and Engineering Applications. **12** (3), 031009 (2019).

[12] Tayebi T., Öztop H. F. Entropy production during natural convection of hybrid nanofluid in an annular passage between horizontal confocal elliptic cylinders. International Journal of Mechanical Sciences. **171**, 105378 (2020).

[13] Asmadi M. S., Md. Kasmani R., Siri Z., Saleh H. Thermal performance analysis for moderate Rayleigh numbers of Newtonian hybrid nanofluid-filled U-shaped cavity with various thermal profiles. Physics of Fluids. **33** (3), 032006 (2021).

[14] Arifin N. M., Saleh H., Hashim I., Azizul F. M. Casson Hybrid Nanofluid Natural Convection in Trapezoidal Cavity containing a Partially Heated Wall. Journal of Advanced Research in Fluid Mechanics and Thermal Sciences. **100** (2), 78–95 (2022).

[15] Asmadi M., Md. Kasmani R., Siri Z., Saleh H., Che Ghani N. Buoyancy-driven heat transfer performance, vorticity and fluid flow analysis of hybrid nanofluid within a U-shaped lid with heated corrugated wall. Alexandria Engineering Journal. **71**, 21–38 (2023).

[16] Alsabery A., Chamkha A., Hussain S., Saleh H., Hashim I. Heatline visualization of natural convection in a trapezoidal cavity partly filled with nanofluid porous layer and partly with non-Newtonian fluid layer. Advanced Powder Technology. **26** (4), 1230–1244 (2015).

Вплив форми наночастинок на природну конвекцію в гібридному нанофлюїді всередині квадратної порожнини

Мохд Алі Ханафія М. А.[1], Аб Гані А.[1], Хафідзуддін М.Е.Х.[1,2],
Мд Аріфін Н.[1*], Мохамад Сом М. Н.[1,2]

[1] *Факультет математики та статистики, Університет Путра Малайзії, 43400 Серданг, Селангор, Малайзія*
[2] *Центр фундаментальних досліджень у галузі науки Університету Путра Малайзії, 43400 Серданг, Селангор, Малайзія*

Чисельно досліджено природну конвекцію в квадратній порожнині з гібридним нанофлюїдом Al_2O_3-Cu/вода з врахуванням впливу форми наночастинок. Основні диференціальні рівняння в частинних похідних з відповідними граничними умовами перетворено в безрозмірні, а потім розв'язано за допомогою методу скінченних елементів. Характеристики потоку та теплопередачі були графічно проілюстровані та пояснені для різних параметрів об'ємних часток наночастинок та параметрів форми наночастинок із середніми числами Нуссельта. Помічено, що вплив різних форм наночастинок полягає в тому, що зі збільшенням емпіричного коефіцієнта форми наночастинок m збільшується загальна площа поверхні наночастинки. Це призводить до того, що більше тепла може розсіюватися, і, у свою чергу, створюється більша швидкість теплопередачі.

Ключові слова: *природний конвекційний потік; гібридний нанофлюїд Al_2O_3-Cu/вода; квадратна порожнина; метод скінченних елементів; форма наночастинок.*